

Title	Liquid-phase explosive crystallization of electron-beam-evaporated a-Si films induced by flash lamp annealing
Author(s)	Ohdaira, Keisuke; Matsumura, Hideki
Citation	Journal of Crystal Growth, 362: 149-152
Issue Date	2011-11-25
Type	Journal Article
Text version	author
URL	http://hdl.handle.net/10119/10882
Rights	NOTICE: This is the author's version of a work accepted for publication by Elsevier. Keisuke Ohdaira, Hideki Matsumura, Journal of Crystal Growth, 362, 2011, 149-152, http://dx.doi.org/10.1016/j.jcrysgr.2011.11.028
Description	

Liquid-phase explosive crystallization of electron-beam-evaporated a-Si films induced by flash lamp annealing

Keisuke Ohdaira^{1,2} and Hideki Matsumura¹

¹Japan Advanced Institute of Science and Technology (JAIST)

²PRESTO, Japan Science and Technology Agency (JST)

We succeed in the formation of micrometer-order-thick polycrystalline silicon (poly-Si) films through the flash-lamp-induced liquid-phase explosive crystallization (EC) of precursor a-Si films prepared by electron-beam (EB) evaporation. The velocity of the explosive crystallization (v_{EC}) is estimated to be ~ 14 m/s, which is close to the velocity of the liquid-phase epitaxy (LPE) of Si at a temperature around the melting point of a-Si of 1418 K. Poly-Si films formed have micrometer-order-long grains stretched along a lateral crystallization direction, and X-ray diffraction (XRD) and electron diffraction pattern measurements reveal that grains in poly-Si films tend to have a particular orientation. These features are significantly different from our previous results: the formation of poly-Si films containing randomly-oriented 10-nm-sized fine grains formed from a-Si films prepared by catalytic chemical vapor deposition (Cat-CVD) or sputtering. One possible reason for the emergence of a different EC mode in EB-evaporated a-Si films is the suppression of solid-phase nucleation (SPN) during FLA due to tensile stress which precursor a-Si films originally hold. Poly-Si films formed from EB-evaporated a-Si films would contribute to the realization of high-efficiency thin-film poly-Si solar cells because of large and oriented grains.

Keywords: A3. Liquid phase epitaxy, A1. Recrystallization, B2. Semiconducting silicon,
B3. Solar cells, A1. X-ray diffraction, A1. Stresses

1. Introduction

The crystallization of precursor amorphous silicon (a-Si) films through non-thermal equilibrium rapid annealing has attracted considerable attentions since it is capable of forming device-grade polycrystalline Si (poly-Si) films on low-cost substrates with poor thermal tolerance [1-10]. Pulse duration for the crystallization is significantly important in order to fully heat and crystallize precursor a-Si films and to suppress thermal damage onto entire glass substrates, especially when thick ($>1\ \mu\text{m}$) a-Si films are used as precursor films with the aim of solar cell application. We have so far investigated the crystallization of a-Si films using flash lamp annealing (FLA), millisecond-order flash discharge from Xe lamps [3,5,6]. Thanks to its proper annealing duration, $4.5\ \mu\text{m}$ -thick poly-Si films can be formed on glass substrates without serious thermal damage to entire glass substrates [11,12]. We have also confirmed that the crystallization of a-Si films takes place laterally through explosive crystallization (EC), autocatalytic lateral crystallization driven by the release of latent heat [13]. We have observed that the flash-lamp-induced EC of catalytic-chemical-vapor-deposited (Cat-CVD) or sputtered a-Si films leads to the formation of poly-Si films containing randomly-oriented, 10-nm-sized fine grains as well as a few hundred nm-sized relatively large grains [13]. Although the actual operation of solar cells fabricated using the FLC poly-Si films has been confirmed [14], their performance is insufficient at present. One approach to improve solar cell properties is to decrease defects in poly-Si films by enlarging grains, for which the suppression of frequent SPN is required.

In this study, we have newly attempted to use μm -order-thick electron-beam- (EB-) evaporated a-Si films as precursor films, and observed the evidences of

liquid-phase-epitaxy- (LPE-) dominated EC. The variation of crystallization mechanism results in the formation of at least a few μm -sized grains stretched along a lateral crystallization direction.

2. Experimental details

We first prepared 60-nm-thick Cr films on $20\times 20\times 0.7\text{ mm}^3$ quartz glass substrates in order to suppress Si film peeling during FLA. About 3 μm -thick a-Si films were deposited on Cr-coated substrates by EB evaporation under a pressure of $4.2\times 10^{-4}\text{ Pa}$ and at a substrate temperature of 200 °C. We then performed FLA onto each a-Si film under stage pre-heating by a halogen lamp at 500 °C. The FLA system supplies a quasi-millisecond pulse consisting of discrete sub-pulses at emitted tunable frequencies of 1-10 kHz [15]. We have confirmed that the quasi-millisecond pulse can induce the crystallization of a-Si films equivalent to conventional single-pulse FLA [15]. Furthermore, the cyclic temperature modulation of Si films induced by discrete pulses during quasi-millisecond pulse emission results in the formation of macroscopic stripe patterns on flash-lamp-crystallized (FLC) poly-Si films, the interval of which yields the velocity of EC (v_{EC}) [15]. The crystallization of a-Si films was evaluated by Raman spectroscopy and X-ray diffraction (XRD). The microstructures of FLC poly-Si films were characterized by differential interference contrast microscopy, transmission electron microscopy, and electron diffraction.

3. Results and discussion

Figure 1(a) shows the surface of a FLC poly-Si film formed by multi-pulse FLA at a sub-pulse emission frequency of 1 kHz. We can see the clear indication of lateral

crystallization along a direction indicated by an arrow in the figure. One can also see boundary lines formed due to the emission of discrete pulses. We can estimate the v_{EC} of the a-Si film to be ~ 14 m/s from these surface macroscopic patterns. Figure 1(b) shows the optical microscopic image of the FLC poly-Si film. Unlike the surface of FLC poly-Si films formed from Cat-CVD or sputtered a-Si films [13], no remarkable surface structures are seen, except for several cracks.

Figure 2 shows the Raman spectrum of a FLC poly-Si film formed from an EB-evaporated a-Si film. The spectrum of a FLC poly-Si film formed from a Cat-CVD a-Si film is also shown for comparison. A FLC poly-Si film formed from an EB-evaporated a-Si film shows a narrower c-Si peak with a full width at half maximum (FWHM) of ~ 4.5 cm^{-1} . This value is close to that of a c-Si wafer of ~ 4 cm^{-1} , and much smaller than that of a FLC poly-Si film formed from a Cat-CVD a-Si film of ~ 7 cm^{-1} . These facts mean that the use of EB-evaporated a-Si films leads to the formation of larger grains. It should also be noted that the c-Si peak of the FLC poly-Si film formed from an EB-evaporated a-Si film locates at lower Raman shift than that of stress-free c-Si of 520.5 cm^{-1} , meaning the existence of tensile stress in this poly-Si film. This fact is consistent with the formation of cracks shown above.

Figure 3 shows the XRD rocking curves of a FLC poly-Si film formed from an EB-evaporated a-Si film. We cannot find any peaks if we do not optimize ψ and ω angles, meaning that grains in the poly-Si have a specific orientation. The grain size of the poly-Si estimated from the Scherrer's equation [16] is ~ 100 nm, which is much larger than that of FLC poly-Si films formed from Cat-CVD a-Si films of 20-30 nm which is obtained in the same method.

Figure 4(a) shows the cross-sectional bright-field TEM image of a FLC poly-Si

film formed from an EB-evaporated a-Si film. The cross-section was formed along a lateral crystallization direction. One can see at least a few μm -long grains stretching to the lateral crystallization directions. The size of grains in depth direction is around 100 nm, which is in good agreement with the estimation based on the XRD results. It should be emphasized that no 10-nm-sized fine grains are seen in the poly-Si film, unlike the case of FLC poly-Si films formed from Cat-CVD or sputtered a-Si films [13,17,18]. Figure 4(b) shows the dark-field TEM images of the FLC poly-Si film. Bright-colored grains are accumulated in the right-hand side of the figure, which means that the orientations of grains are considerably aligned in this region. Figure 5 shows the electron diffraction pattern of the poly-Si film, indicating aligned spot patterns like single-crystalline Si. This pattern is significantly different from that of FLC poly-Si films formed from Cat-CVD or sputtered a-Si films, showing typical multi-ring patterns which indicate the formation of randomly-oriented multi-grains [17,18].

These features for the FLC poly-Si formed from EB-evaporated a-Si films shown above indicate that lateral epitaxial growth compete with nucleation process, unlike the case of using Cat-CVD or sputtered films as precursor films. The v_{EC} of 14 m/s can be quantitatively explained if we consider LPE of Si at a temperature around the melting point of a-Si of 1418K [5]. The v_{EC} estimated is also quite close to the value in a previous report of laser-induced LPE-based EC by Geiler *et al* [7]. Therefore, we can conclude that the EC observed in EB-evaporated a-Si films is dominated by LPE. The lateral extension of grains, shown in Fig. 4, is probably due to large temperature gradient along a lateral crystallization direction during EC.

One possible reason for the emergence of different crystallization mechanisms is the film stress of precursor a-Si films. According to our results, Cat-CVD and

sputtered films, which have compressive stress, are converted to poly-Si films with solid-phase-nucleated 10-nm-sized fine grains [17,18], while the use of EB-evaporated films, with tensile stress, results in the emergence of LPE-dominated EC as shown above. It is known that compressive stress in a-Si can enhance SPN [19]. Geiler *et al.* also used precursor a-Si films formed by ultra-high-vacuum evaporation [7]. Although they have shown no data about the stress of precursor films, the a-Si films may also have tensile stress because of the nature of evaporated a-Si films [20]. These facts mean that the stress of precursor a-Si films might be quite important to control the mechanism of EC and the microstructures of poly-Si films formed. Further investigation is necessary to clarify the effects of film stress on the crystallization mechanisms. From the viewpoint of the application of poly-Si films to solar cells, the properties of FLC poly-Si films formed from EB-evaporated a-Si films, larger and more oriented grains, are desirable. For the application of FLC poly-Si films formed from EB-evaporated a-Si films to solar cells, however, serious cracking shown in Fig. 1(b) should be suppressed. Thus, also for the suppression of crack generation, the stress control of precursor a-Si films would be important.

4. Summary

We have observed the LPE-dominated EC of EB-evaporated a-Si films. v_{EC} of the a-Si films is estimated to be ~ 14 m/s, which is explainable as the speed of LPE around the melting point of a-Si of 1418 K. FLC poly-Si films formed have at least a few μm -sized grains stretched along a lateral crystallization direction. These features are significantly different from the results of the crystallization of Cat-CVD and sputter precursor a-Si films which we have reported so far, and the effect of stress in precursor

a-Si films can be considered as a possible cause for the emergence of different EC mechanisms.

Acknowledgment

The authors acknowledge T. Yoshida and L. Yang for their FLA experiment. We also would like to acknowledge Ulvac Inc. for their provision of EB-evaporated a-Si films. This work was supported by JST PRESTO program.

References

- [1] J. S. Im, H. J. Kim, *Appl. Phys. Lett.* 64 (1994) 2303-2305.
- [2] J. Kumar Saha, K. Haruta, M. Yeo, T. Koabayshi, H. Shirai, *Sol. Energy Mat. Sol. Cells* 93 (2009) 1154-1157.
- [3] B. Pécz, L. Dobos, D. Panknin, W. Skorupa, C. Lioutas, N. Vouroutzis, *Appl. Surf. Sci.* 242 (2005) 185-191.
- [4] C. C. Kuo, W. C. Yeh, J. B. Chen, J. Y. Jeng, *Thin Solid Films* 515 (2006) 1651-1657.
- [5] M. Smith, R. McMahon, M. Voelskow, D. Panknin, W. Skorupa, *J. Cryst. Growth* 285 (2005) 249-260.
- [6] S. Saxena, D. C. Kim, J. H. Park, J. Jang, *IEEE Electron Dev. Lett.* 31 (2010) 1242-1244.
- [7] H. D. Geiler, W. Glaser, G. Gotz, M. Wagner, *J. Appl. Phys.* 59 (1985) 3091-3099.
- [8] G. Auvert, D. Bensahel, A. Perio, V. T. Nguyen, G. A. Rozgonyi, *Appl. Phys. Lett.* 39 (1981) 724-726.
- [9] D. Bensahel, G. Auvert, A. Perio, and J. C. Pfister, A. Izrael, P. Henoc, *J. Appl. Phys.* 54 (1983) 3485-3488.
- [10] B. Loisel, B. Guenais, A. Poudoulec, P. Henoc, *Thin Solid Films* 117 (1984) 117-123.
- [11] K. Ohdaira, Y. Endo, T. Fujiwara, S. Nishizaki, and H. Matsumura, *Jpn. J. Appl. Phys.* 46, 7603-7606 (2007).
- [12] K. Ohdaira, T. Fujiwara, Y. Endo, S. Nishizaki, H. Matsumura, *Jpn. J. Appl. Phys.* 47 (2008) 8239-8242.
- [13] K. Ohdaira, T. Fujiwara, Y. Endo, S. Nishizaki, H. Matsumura, *J. Appl. Phys.* 106

(2009) 044907-1-8.

- [14] Y. Endo, T. Fujiwara, K. Ohdaira, S. Nishizaki, K. Nishioka, H. Matsumura, *Thin Solid Films* 518 (2010) 5003-5006.
- [15] K. Ohdaira, N. Tomura, S. Ishii, H. Matsumura, *Electrochem. Solid State Lett.* 14 (2011) H372-H374.
- [16] P. Scherrer, *Nachr. Ges. Wiss. Göttingen*, 26 September (1918) 98-100.
- [17] K. Ohdaira, S. Ishii, N. Tomura, H. Matsumura, *Jpn. J. Appl. Phys.* 50 (2011) 04DP01-1-3.
- [18] K. Ohdaira, S. Ishii, N. Tomura, H. Matsumura, *J. Nanosci. Nanotech.* (in press).
- [19] H. Fujiwara, M. Kondo, A. Matsuda, *Jpn. J. Appl. Phys.* 41 (2002) 2821-2828.
- [20] J. Kim, D. Inns, D. K. Sadana, *Thin Solid Films* 518 (2010) 4908-4910.

Figure captions

Figure 1 (a) Surface image and (b) optical microscopic image of a FLC poly-Si film formed from an EB-evaporated a-Si film at a sub-pulse emission frequency of 1 kHz.

Figure 2 Raman spectrum of a FLC poly-Si film formed from an EB-evaporated a-Si film. The spectrum of a FLC poly-Si film formed from a Cat-CVD a-Si films is also shown for comparison.

Figure 3 XRD rocking curves of a FLC poly-Si film formed from an EB-evaporated a-Si film taken under different $\Delta\omega$ and ψ angles.

Figure 4 Cross-sectional (a) bright-field and (b) dark-field TEM images of a FLC poly-Si film formed from an EB-evaporated a-Si film. A circle in the bright-field image is the measurement position of an electron diffraction pattern shown in Fig. 5. Arrows indicate a lateral crystallization direction.

Figure 5 Electron diffraction pattern of a FLC poly-Si film formed from an EB-evaporated a-Si film.

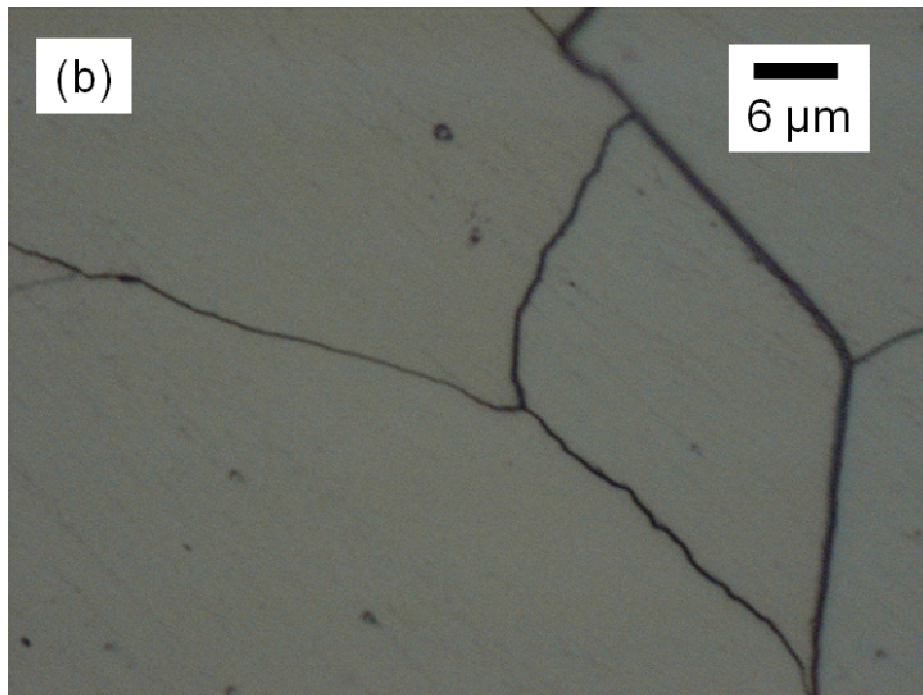
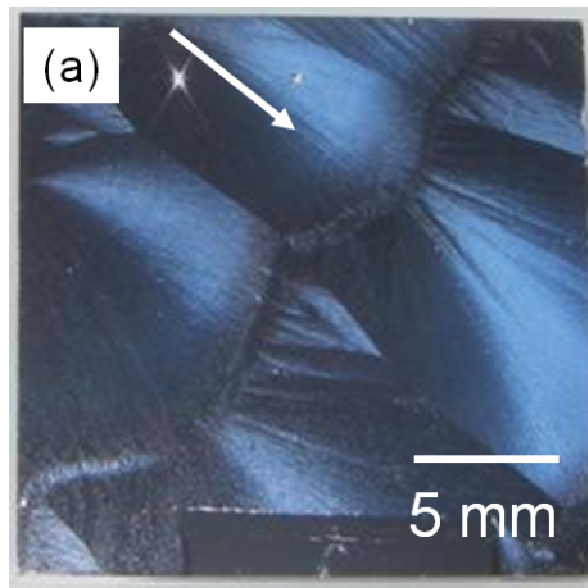


Figure 1 K. Ohdaira *et al.*,

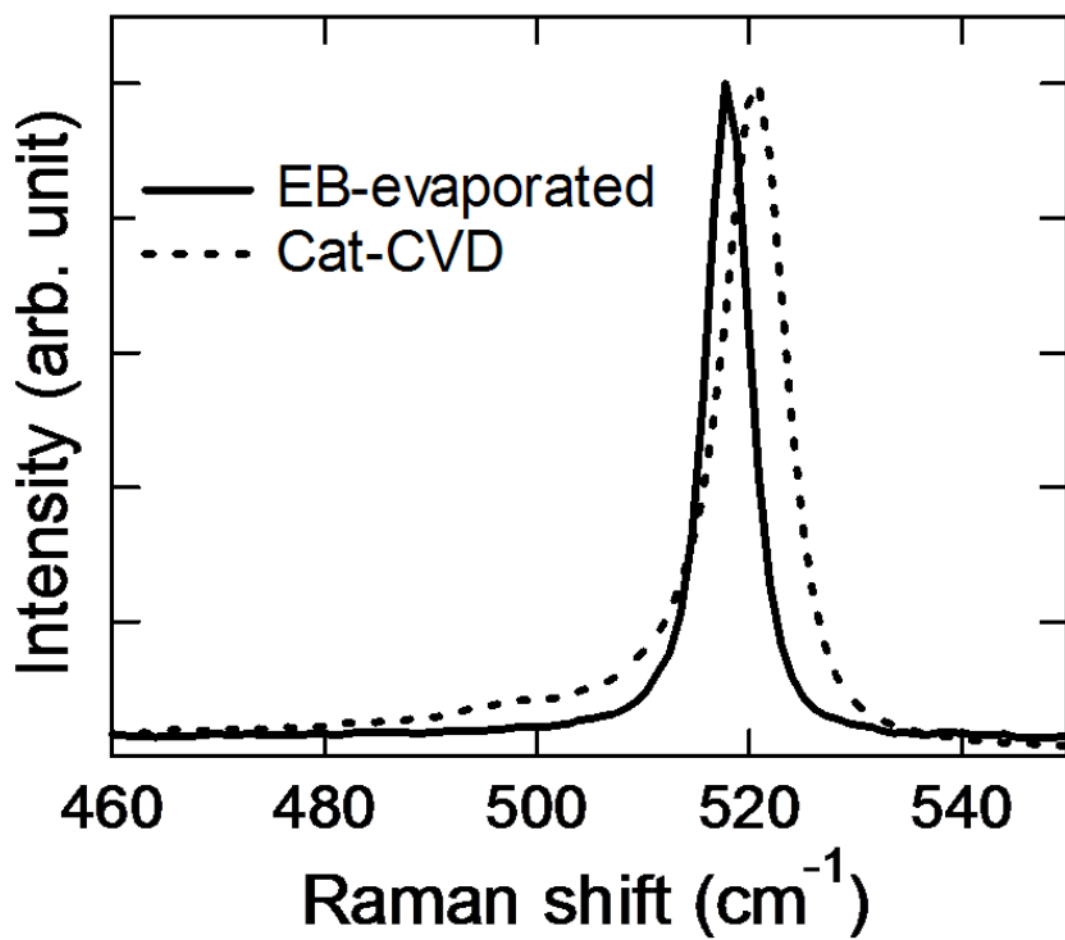


Figure 2 K. Ohdaira *et al.*,

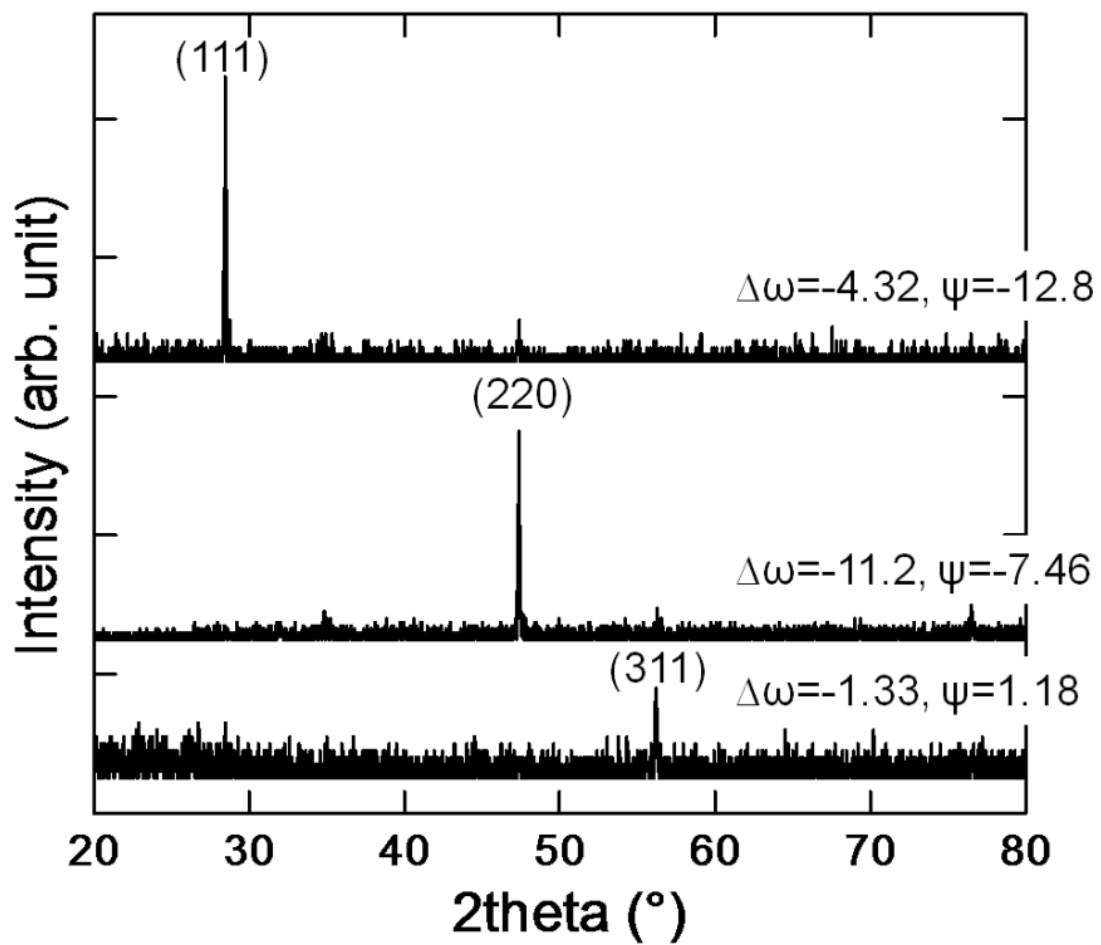


Figure 3 K. Ohdaira *et al.*,

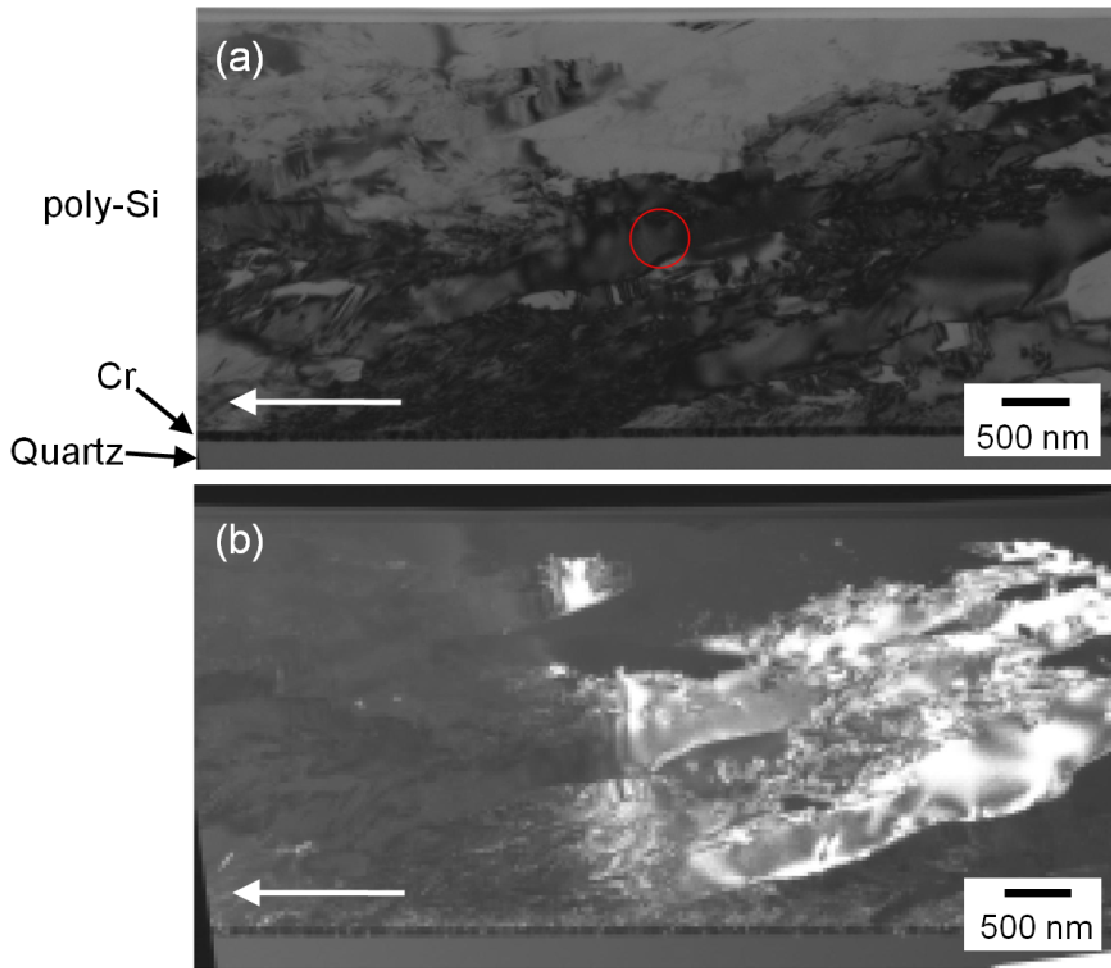


Figure 4 K. Ohdaira *et al.*,

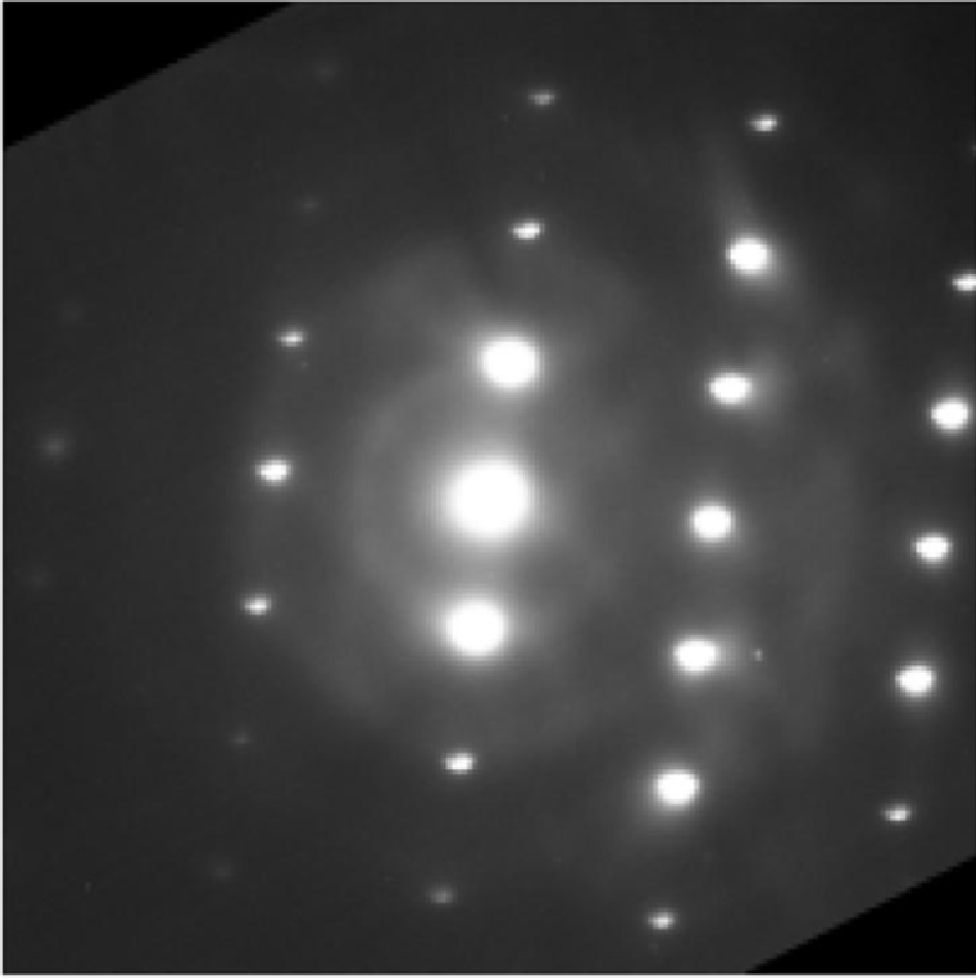


Figure 5 K. Ohdaira *et al.*,